A&A 389, 191–201 (2002)
DOI: 10.1051/0004-6361:20020606

Astronomy & Astrophysics

Measuring magnetic fields of early-type stars with *FORS1* at the *VLT*⋆

S. Bagnulo[1], T. Szeifert[1], G. A. Wade[2], J. D. Landstreet[3], and G. Mathys[1]

[1] European Southern Observatory, Casilla 19001, Santiago 19, Chile
e-mail: sbagnulo@eso.org, tszeifer@eso.org, gmathys@eso.org
[2] Department of Physics, Royal Military College of Canada, PO Box 17000, Station "Forces" Kingston, Ontario, Canada K7K 7B4
e-mail: Gregg.Wade@rmc.ca
[3] Physics & Astronomy Department, The University of Western Ontario, London, Ontario, Canada N6A 3K7
e-mail: jlandstr@astro.uwo.ca

Received 15 January 2002 / Accepted 12 March 2002

Abstract. This paper describes an experiment aimed at evaluating the capability of the *FORS1* instrument at the *VLT* for measuring weak (≃0.1%) Zeeman circular polarization signatures in stellar H Balmer lines. We have obtained low-resolution polarized spectra at 3500–5800 Å of two bright A-type stars, HD 94660, and HD 96441. The former is a well known magnetic star, the latter an apparently non-magnetic, unpolarized star that was observed for comparison purposes. In order to test the possibility of performing multi-object spectropolarimetric measurements (e.g., for cluster studies), observations were taken both on-axis (i.e., at the CCD field center) and off-axis (i.e., at the edges of the CCD). In HD 94660 (the magnetic star), we detected a clear signal of circular polarization in all observed hydrogen Balmer lines (i.e., from Hβ to the Balmer limit), with a typical peak-to-peak amplitude of about 0.8%. From the analysis of Stokes V under the weak-field approximation, we have estimated a mean longitudinal field of -2085 ± 85 G, a value fully consistent with previous studies of this star. Notably, we found that at wavelengths shorter than about 4100 Å, the polarization signal detected off-axis is about 20–30% smaller than that detected on-axis. No polarization due to the Zeeman effect was detected in the comparison star HD 96441, and we estimate that the contribution due to instrumental circular polarization is limited to the order of 0.01%. This experiment demonstrates the effectiveness of *FORS1* at the *VLT* as a tool for high-sensitivity diagnosis of the magnetic field in upper main sequence stars, providing the potential for measuring fields in fainter and more rapidly rotating stars than has previously been possible.

Key words. stars: magnetic fields – polarization – stars: chemically peculiar – stars: individual: HD 94660 – stars: individual: HD 96441

1. Introduction

Magnetic fields may well represent the most important agent of structure and variability in stellar outer layers. Such fields have been firmly detected in stars occupying most regions of the Hertzsprung-Russell diagram: in pre-main sequence stars (Johns-Krull et al. 1999), in late type stars (Robinson et al. 1980), and in white dwarfs (Kemp et al. 1970; Schmidt & Smith 1995). Arguably, the most potentially productive objects for studies of stellar magnetism are the chemically peculiar stars of the upper main sequence (the Ap/Bp stars and their kin), that possess strong, organised magnetic fields that are relatively easy to detect, measure and model. Because many Ap/Bp stars have bright apparent magnitudes, most observations that presently exist have been obtained using small telescopes with diameters less than 4 m (the 6 m telescope at the Russian Special Astrophysical Observatory is a notable exception).

Little attention has been paid, however, to exploiting the new generation of large telescopes for stellar magnetic field studies. In fact, no high-resolution spectropolarimetric capabilities are available on any of the 8 m class telescopes, discouraging observers from using large telescopes for detailed studies of magnetic stars.

The Unit 1 *Antu* of the ESO *VLT* is equipped with *FORS1*, a multi-mode spectrograph with a polarimetric capability allowing the acquisition of low resolution spectra ($R \lesssim 2000$) in all four Stokes parameters[1]. The spectropolarimetric mode of *FORS1* was originally designed

Send offprint requests to: S. Bagnulo,
e-mail: sbagnulo@eso.org

⋆ Based on observations obtained at the *VLT* within the context of DDT 266.D-5649.

[1] At the moment of writing, *FORS1* is temporarily mounted at the Unit 3 *Melipal*.

to be used mainly for detection of relatively strong polarization signals in faint objects, e.g., to study the multi-MegaGauss magnetic fields of some white dwarfs. In this paper we describe a pilot experiment that we have performed aimed at determining if *FORS1* may also be used for the detection of comparatively *weak* magnetic fields, such as those of the Ap/Bp stars. Such fields produce polarization signatures in spectral lines with amplitudes of a few tenths of a percent or less. With this aim, we have obtained low-resolution spectropolarimetry of the H Balmer series from Hβ to the Balmer limit of two main sequence A-type stars. One target, HD 94660, is a well studied magnetic Ap star, characterised by a nearly constant longitudinal magnetic field of about -2 kG. The second target is an apparently non-magnetic and unpolarized star that was observed for comparison purposes, in particular to give an accurate estimate of the instrumental circular polarization.

This paper is organised as follows. Section 2 describes how the magnetic field can be determined from observations of polarized spectra of H Balmer lines. Section 3 describes the observing technique and data reduction procedure, and Sect. 4 presents the results. In Sect. 5 we discuss which perspectives our results open for observations of stellar magnetic fields with large telescopes.

2. Theoretical basis

Most of our knowledge of stellar magnetic fields comes from the detection of *circular* polarization of *metallic* lines via medium-high resolution ($R \gtrsim 20\,000$) spectropolarimetric measurements. The theory of spectral line formation in a magnetic atmosphere shows that the splitting of a spectral line observed in both senses of circular polarization is proportional to the component of the magnetic field along the line of sight averaged over the stellar disk, i.e., the *mean longitudinal magnetic field* (Babcock 1947, 1958). This method for determining the longitudinal field is often referred to as the *photographic* technique.

An alternative technique for the detection of stellar magnetic fields was developed in the 70's by Angel & Landstreet (1970; see also Borra & Landstreet 1980), based on the detection of circular polarization in hydrogen Balmer lines (and in some hot stars, also He lines). Similar to the measurement of the Zeeman splitting of spectral lines observed in opposite senses of circular polarization, the measurement of the difference between the circular polarization observed in the red and blue wings of, e.g., Hβ, permits one to derive the mean longitudinal field. Let us define:

$$C_z = \frac{e}{4\pi m_{\rm e} c^2} \qquad (\simeq 4.67 \times 10^{-13}\,\text{Å}^{-1})$$

where e is the electron charge, $m_{\rm e}$ the electron mass, c the speed of light. For a spectral line formed in a Milne-Eddington atmosphere, and in the so-called *weak-field* regime (i.e. when the Zeeman splitting is small compared to the line intrinsic broadening), one can show that:

$$\frac{V}{I} = -g_{\rm eff}\ C_z\ \lambda^2\ \frac{1}{I}\ \frac{{\rm d}I}{{\rm d}\lambda}\ \langle \mathcal{B}_z \rangle\ , \qquad (1)$$

where $g_{\rm eff}$ is the effective Landé factor, V is the Stokes parameter which measures the circular polarization, I is the usual (unpolarized) intensity, λ is the wavelength expressed in Å, and $\langle \mathcal{B}_z \rangle$ is the mean longitudinal field expressed in G. In A and B stars, for spectral lines of iron-peak elements (which have typical intrinsic line widths $\lesssim 3$ km s^{-1}), the weak-field regime typically holds only for magnetic strengths less than about 1 kG. Hydrogen lines are characterised by a much larger intrinsic broadening than metallic lines, and the weak-field approximation can be reasonably adopted for magnetic strengths up to a few tens of kG.

An additional advantage is that the H Balmer lines are so broad that they can be easily detected even at low resolution. In fact, Borra & Landstreet (1980) used a *photopolarimetric* technique, which made use of two 5 Å-wide interference filters centred on the wings of the Hβ. However, the validity of Eq. (1) is not fully established on theoretical grounds. On the one hand, it rests on a description of the line formation accounting only for the Zeeman splitting of the atomic levels, while actually there are also significant contributions of the strong linear Stark effect due to the surrounding charged particles and, possibly, of the Lorentz effect due to the thermal motion of the hydrogen atoms in the magnetic field. On the other hand, for interpretation of disk-integrated observations, the treatment of the limb darkening adopted for derivation of this equation is not fully correct. The reader is referred to Mathys et al. (2000) for more details. Other complications may arise from departures from LTE and from the Milne-Eddington approximation. However, the validity of Eq. (1) – to within a certain degree of approximation – has been empirically confirmed by the large bulk of photopolarimetric data of H Balmer lines obtained by Borra & Landstreet (1980), that turned out to provide determinations of the longitudinal field roughly consistent with the estimates obtained with high-resolution spectropolarimetry of metallic lines.

We decided to investigate whether a similar technique could be used with a low resolution spectropolarimeter such as *FORS1* with which, in addition, *several Balmer lines may be observed simultaneously*. Spectropolarimetry of Hα and Hβ Balmer line is commonly applied for detection of strong magnetic fields of white dwarfs (e.g., Schmidt & Smith 1995; Putney 1997). The question was whether we could detect as well much weaker fields, such as those of magnetic Ap stars.

3. Observations

As a target for our experiment we selected a well studied magnetic Ap star, HD 94660 (= HR 4263, $V = 6.1$), which is known to have a very long rotational period ($\simeq$2800 d; Landstreet & Mathys 2000), and a moderately strong

magnetic field ($\langle \mathcal{B}_z \rangle \simeq -2\,\mathrm{kG}$; Landstreet & Mathys 2000). For comparison, we also observed an apparently non-magnetic star of similar spectral type and magnitude, HD 96441 (= HR 4320, $V = 6.8$).

3.1. Instrumental setup

FORS1 (Focal reducer Optical Range Spectrograph), mounted on the 8 m *Antu* telescope of the *VLT* on Cerro Paranal, is a multi-mode instrument equipped with polarization analysing optics comprising super-achromatic half-wave and quarter-wave phase retarder plates, and a Wollaston prism with a beam divergence of 22″ in standard resolution mode. The instrument optics and performance, as well as the operational aspects, are outlined by Seifert et al. (2000) and by Szeifert & Böhnhardt (2001). Among the various grisms currently available, the most suitable ones for our purpose are the *GRISM 600 B*, which covers all H Balmer lines from Hβ to the Balmer jump, and the *GRISM 600 R*, which among H Balmer lines, includes Hα only. They both have 600 grooves mm^{-1}, and, with a slit width of 1″, they give a spectral resolving power of $R = 815$, and $R = 1230$, respectively, for a dispersion of 1.20 Å and 1.08 Å per pixel, respectively. *GRISM 600 V* spans a wavelength interval including Hα and Hβ, but is not available in polarimetric mode. The other grisms available at *FORS1* offer a lower spectral resolution which was deemed insufficient for our purpose (for considerations about the optimal compromise between signal-to-noise ratio and spectral resolution see Landstreet 1982).

Taking into account that for H Balmer lines of A and B stars $1/I \times \mathrm{d}I/\mathrm{d}\lambda$ is typically $<0.1\,\text{Å}^{-1}$, Eq. (1) shows that the expected value of the circular polarization of Hβ is about 10^{-6} per G. This means that in order to measure a magnetic field with a 100 G error bar, we need a S/N ratio higher than 10 000, i.e., we need to count at least 10^8 photons! With the *GRISM 600 B*, *FORS1* spans the entire interval range between 3500 and 5800 Å, which includes all Balmer lines from Hβ on. Assuming that about ten of them are suitable for Zeeman analysis, we estimate that a polarization signal can be detected in a few hundred pixels per row along the dispersion direction. With a *FWHM* of the seeing spatial profile of four pixels, we conclude that the useful polarized signal that we need to detect is distributed over about 10^3 pixels. Therefore, for detection of stellar magnetic fields with a 100 G error bar, one should try to reach a photon count per pixel of the order of 10^5. This is safely possible by setting the CCD readout mode to the lowest possible gain, and with the help of multiple exposures (in fact, 10^5 photons per pixel is close to saturation due to the hardware limits of the digital-analogic converter).

Using *GRISM 600 R* is also an interesting option, virtually equivalent to the choice of *GRISM 600 B*. The polarization signal expected in Hα is almost twice that predicted for Hβ, and the resolution obtained with the *GRISM 600 R* is 50% higher than with *GRIMS 600 B*. Requirements for an ultra-high S/N ratio are somewhat relaxed, and, in order to determine the longitudinal field with an error bar of 100 G, a total photon count of 10^7 photons on the Hα line should suffice. Again, this corresponds to a photon count per pixel $\gtrsim 10^5$.

For the observations presented in this paper we decided to use the *GRISM 600 B*. To reach a compromise between the highest possible spectral resolution and limited slit loss we set the slit width to 0.5″. This corresponds to a resolution of $\lambda/\Delta\lambda \sim 1600$, i.e., about 3 Å at H$\beta$. Clearly, for a 6th magnitude star observed with an 8 m telescope, slit losses are not an important issue, but we decided to test the instrument setup that was deemed the most appropriate for observations of much fainter stars (see Sect. 5).

3.2. Observational strategy

Circular polarization measurements are performed by inserting, into the optical path, the quarter-wave plate and the Wollaston prism. In the ideal case, Stokes V may be obtained by subtracting the photon counts f^{e} in the extra-ordinary beam from the photon counts f^{o} of the ordinary beam. Alternatively, Stokes V may be obtained from the difference of the photon counts either in the ordinary beam, or in the extra-ordinary beam, measured at two different angles of the retarder waveplate separated by 90°. In fact, as we will see later, a combination of exposures taken at different waveplate orientations allows us to minimise the contributions of spurious (instrumental) polarization.

One source of instrumental polarization is the so called *cross-talk* effect, which is related to the fact that the phase shift introduced by the retarder waveplate, ideally 90° in the case of the quarter-wave plate, is in fact a function of wavelength. This makes the photon counts in the ordinary and extraordinary beams proportional not only to the circular polarization of the incoming radiation, but also, through a smaller coefficient, to the linear polarization of the incoming radiation. Linear polarization may result from the Zeeman effect (in the case of the magnetic star), or to the presence, in the interstellar or circumstellar medium, of non-spherical dust grains oriented along a preferred direction. The amount of linear polarization in spectral lines due to the Zeeman effect is typically 5 to 10 times less than the amount of circular polarization due to the same effect. Therefore, in our case, cross-talk with linear polarization due to the Zeeman effect should be negligible. For nearby stars, such as those as we have observed, linear polarization due to the interstellar medium should be <1% (e.g., Leroy 2000). This upper limit may be a non-negligible value, since the amount of circular polarization that we are aiming to detect is as small as a few tenths of one percent. However, linear polarization due to the interstellar medium is continuum polarization, exhibiting a smooth dependence upon wavelength. Therefore, cross-talk with linear polarization due to the interstellar medium should manifest itself at worst as a small

overall offset (<0.1%) of the Stokes V. Recalling that our interest is concentrated toward the *difference* of circular polarization observed in the wings of the Hydrogen lines, we conclude that the impact of the cross-talk effect on the observations of circular polarization presented in this paper should be minimal. We nevertheless decided to adopt an observing strategy that minimizes the cross-talk effect; the *FORS1* manual (Szeifert & Böhnhardt 2001; see also Semel et al. 1993) states that this effect cancels out to the first order by obtaining Stokes V as

$$\frac{V}{I} = \frac{1}{2}\left\{ \left(\frac{f^{\rm o} - f^{\rm e}}{f^{\rm o} + f^{\rm e}}\right)_{\alpha=-45^\circ} - \left(\frac{f^{\rm o} - f^{\rm e}}{f^{\rm o} + f^{\rm e}}\right)_{\alpha=+45^\circ} \right\}, \quad (2)$$

where α indicates the nominal value of the position angle of the retarder waveplate, i.e., the angle counted counterclockwise between the North Celestial Meridian and the fast axis of the quarter waveplate (see Landi Degl'Innocenti 1992). Obtaining Stokes V through Eq. (2) permits one also to minimize the impact of an imperfect flat-fielding correction. We thus adopted an observing sequence consisting of exposures with retarder waveplate angles +45°, +45°, −45°, −45°, +45°, +45°, −45°, −45°.

To study the performance for further multi-object Stokes V observations, we have observed both targets on-axis, i.e., in the center of the field, and off-axis with a 180″ offset to the edge of the field. The telescope was offset toward the north for HD 94660, and toward the South for HD 96441.

3.3. Observations and data reduction

Observations of the magnetic star HD 94660 were obtained between March 22, 2001 at UT 23:54 and March 23, 2001 at UT 00:29. The non-magnetic comparison star HD 96441 was observed on March 25 between UT 00:08 and UT 01:24. For HD 94660, the Heliocentric Julian Dates corresponding to the middle of the observations are HJD = 24551991.499 and 2451991.513 for the on-axis and the off-axis exposures, respectively. For HD 96441 they are HJD = 24551993.507 (on axis) and 24551993.548 (off-axis). The exposure times were 3.4 and 6.8 s for the on- and off-axis measurements of HD 94660, respectively, and 10 and 20 s for the on- and off-axis measurements of the comparison star HD 96441.

Flat field and wavelength calibrations were taken during day time with the telescope pointed at the zenith, for the two different retarder waveplate setups ($\alpha = -45^\circ$ and $+45^\circ$) used for the observations. A unique (normalised) master flat field was calculated from the median flux of all flat fields taken with the retarder quarter-wave plate at -45° and at $+45^\circ$. The stellar spectra were extracted from the flat-field corrected frames as a plain sum over about ten CCD rows for each beam. (Optimal extraction techniques would not bring any significant gain for such high S/N spectra.) Wavelength calibration was then performed by associating with each individual science spectrum the calibration frame obtained with a similar orientation of the retarder waveplate. Ordinary and extraordinary beams were independently calibrated with the corresponding beams of the reference spectrum. (A posteriori it was found that adopting an identical dispersion law for both the ordinary and extraordinary beam, and for both orientations of the retarder waveplate, we would obtain very similar results.) For the very short exposures taken here, the fine tuning of wavelength calibration based on night sky lines could not be performed. Therefore the accuracy of the wavelength calibration is restricted by instrument flexures, which are expected from commissioning data to be less then 0.9 pixels at the zenith distance z corresponding to the night-time observations ($z = 45^\circ$ to 49°). Numerical experiments show that this is of negligible impact on the determination of the mean longitudinal magnetic field (see Sect. 4.2).

Stokes V/I was finally obtained from Eq. (2), whereas Stokes I was obtained as a sum over all beams.

4. Results

4.1. Observed Stokes I and V profiles

Figure 1 shows the spectrum of HD 94660 observed in "natural" light (Stokes I), normalised to the (pseudo) continuum, together with the spectrum of the circularly polarized radiation. Solid lines refer to the Stokes profiles observed on-axis, dotted lines to the Stokes profiles observed off-axis. The Stokes I observed off-axis has been superimposed on the Stokes I observed on-axis, while Stokes V taken off-axis has been shifted by −0.3% with respect to Stokes V measured on-axis.

The observed Stokes I spectrum is characterised by about a dozen Balmer lines, and by numerous weak, high frequency signatures. Our spectra were obtained with an ultra-high S/N ratio; the S/N ratio calculated at $\lambda = 4750{-}4800$ Å as the square root of the photon counts per pixel (binned along the slit direction) is 1700 on-axis, and 2000 off-axis. Furthermore, it should be noted that the spectrum taken on-axis appears almost exactly superimposed on the spectrum obtained off-axis. Accordingly, high-frequency Stokes I variability cannot be interpreted in terms of random photon noise, but represents the contribution of many unresolved metallic absorption lines. This feature hardly comes as a surprise – spectra extremely rich in metal lines are typical of chemically peculiar stars, and reflect large overabundances (with respect to the sun) of iron-peak and rare-earth elements. On the other hand, the 3934 Å Ca II line of HD 94660 appears much weaker than that of HD 96441 (see Fig. 2), a chemically normal star of similar spectral type. Again, this is consistent with the fact that many chemically peculiar stars appear calcium-deficient with respect to other stars of similar spectral type.

The sole discrepancy between on-axis and off-axis Stokes I observations occurs in the spectral range ≃4020–4100 Å (i.e., approximately in the blue wing of Hδ). This is due to a zero-order back reflection within the

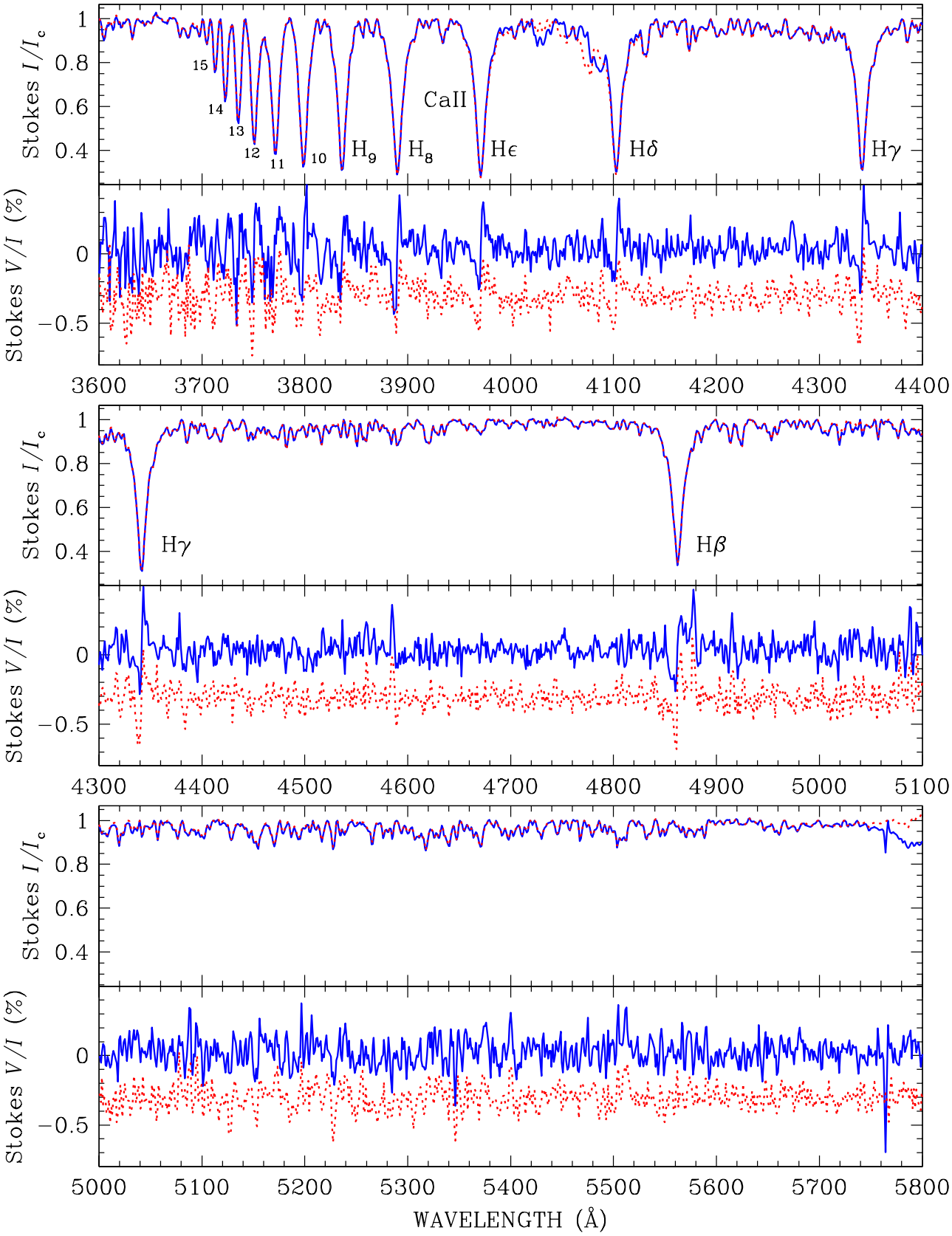

Fig. 1. The polarized spectrum of the magnetic Ap star HD 94660. Solid lines show the Stokes profiles obtained in the field centre, dotted lines refer to the data obtained with a telescope offset of 180″ to the north (the star appeared thus close to the bottom edge of the field); Stokes I profiles are superimposed, Stokes V observed off-axis is shifted to −0.30% with respect to Stokes V observed on-axis for display purposes. The consistency of the Stokes I and V spectra taken on-axis and off-axis implies that the various high-frequency features are real, i.e., due to the contributions of many non resolved lines.

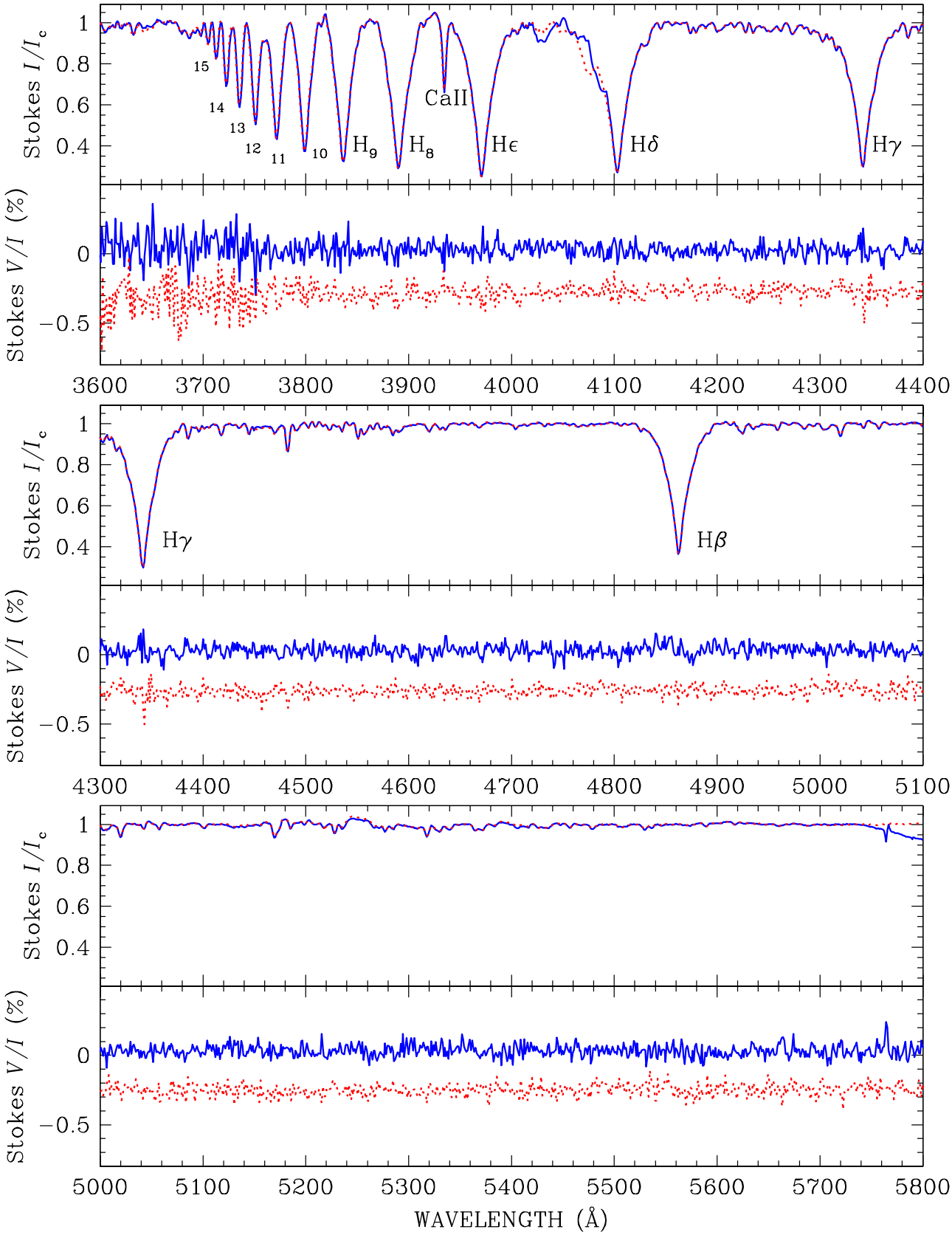

Fig. 2. The unpolarized spectrum of the non magnetic A star HD 96441. Solid lines show the Stokes profiles obtained in the field centre, dotted lines refer to the data obtained with a telescope offset to 180 arcsec to the south, i.e., the stellar spectrum was located close the the top edge of the CCD field. The high-frequency features observed in the Stokes V taken on-axis are not consistent with those observed in the Stokes V observed off-axis, and, as such, should be ascribed to random photon-noise.

instrument, characteristic of *GRISM 600 B* only. This reflection normally does not strongly affect science spectra, but flat fields are contaminated, and, in order to obtain a more reliable Stokes I profile from off-axis observations, we point out that one should not flat-field the spectral region close to the blue wing of Hδ (however at the expense of a lower S/N ratio). All H Balmer lines appear polarized up to a maximum level of about 0.4% (which corresponds to a peak-to-peak variation of 0.8%). Note the characteristic S-shape of Stokes V profiles of Balmer lines; the fact that the circular polarization is negative in the blue wings and positive in the red wings tells us that the mean longitudinal field is negative, i.e., points away from the observer.

Like Stokes I, Stokes V also appears very noisy. Again, since the high-frequency Stokes V variability observed on-axis is fully consistent with that detected off-axis, one can conclude that a substantial fraction of the "noise" is in fact due to the polarization coming from the metallic lines.

The strategy adopted for observations and data reduction largely minimizes the impact on Stokes V of an incorrect flat-fielding near Hδ, and no large differences are detected in this wavelength region in the *shape* of Stokes V as observed on- and off-axis. A more remarkable overall inconsistency appears in the *amplitude* of Stokes V at all wavelengths shorter than about 4100 Å. Stokes V profiles detected off-axis appear weaker than those measured on-axis. For instance, the peak-to-peak amplitude of Hϵ in Stokes V measured off-axis is about 20% less than that measured on-axis. The reasons for this phenomenon are not fully clear to us. One could hypothesize that the spectral resolution in the bluer part of the spectrum is lower for observations taken at the edges of the field than at the field centre, so that Stokes V appears more smeared out off-axis than on-axis. However, the full consistency of Stokes I observations off- and on-axis invalidates this explanation. The reasons for this phenomenon of "off-axis depolarization" should be sought in the polarimetric optics.

Although both the retarder waveplate and Wollaston prism are located in the parallel beam, the off-axis beam is in fact tilted by a few degrees with respect to the on-axis beam, resulting in a slightly longer optical path through the retarder. Consequently, the retardation angle introduced by the quarter-wave plate in the off-axis beam is different from that introduced in the on-axis beam. Furthermore, from *FORS1* commissioning studies it is known that – at wavelengths shorter than 4100 Å – the retardation angle of the *half*-wave plate deviates from the nominal value by a few degrees. If a similar problem exists for the *quarter*-wave plate, it is conceivable that this combination of instrumental features could be responsible for the observed discrepancy between the on- and off-axis polarizations. However, our observational strategy should be fairly robust. Numerical simulations show that a 30% discrepancy in the peak-to-peak Stokes V profile can be accounted for only by assuming a 30°−40° deviation of the retardation angle from its nominal value of 90°. As a matter of fact, it is hard to justify such a large deviation, even for the most extreme off-axis beam (in *FORS1*, a reasonable upper limit for the tilt angle of the off-axis beam is 5°).

On the other hand, it should be taken into account that, due to the large size of the parallel beam (138 mm), the retarder plates are composed of a 3×3-mosaic of smaller plates (that were aligned within 0.1° with respect to each other in the laboratory). A possible (but untested) explanation is that shading of the mosaic support structure, as well as internal scattered light and reflection from the polarization optics, might be responsible for the observed off-axis depolarization, in a way that we are not able to describe precisely.

In conclusion, we have detected a stronger polarization at the field center than at field edge, but we are unable to identify why this is so. However, it should be pointed out that the observations presented in this paper are not the most appropriate ones to investigate this problem. In fact we are dealing with a polarization signal of a few tenths of one percent in spectral regions with a comparatively low S/N ratio. A more conclusive experiment could target a *strongly* circularly polarized source (e.g., a strongly magnetized white dwarf), which would permit us to better quantify the phenomenon. A better understanding could be obtained by performing observations with various offsets, both in imaging polarimetry and spectropolarimetry. Stokes Q and U observations could also possibly help. If linear polarization did not show the same loss of signal off-axis, this would strengthen the suspicion that the quarter-wave plate is at the origin of the problem.

Figure 2 shows the observations of HD 96441, the non-polarized star that was selected as a comparison star. The S/N ratio, calculated as described before for HD 94660, is about 2500 for both on- and off-axis observations. The spectrum appears far less metal-rich than in the case of HD 94660 (except that the Ca II line at 3834 Å appears much deeper than in HD 94660). As with HD 94660, Stokes I obtained off-axis differs from Stokes I observed off-axis in the blue wing of Hδ, but is otherwise effectively identical. No polarization is detected around the Balmer lines, and a comparison between Stokes V observations taken off-axis with those taken on-axis suggests that the observed variability of the circular polarization signal should be ascribed mostly to random photon noise.

4.2. Determining the mean longitudinal magnetic field

A least-square technique was used to derive the longitudinal field via Eq. (1), allowing also for a constant contribution related to the instrumental polarization (i.e., as a zero-order term in a first-order polynomial interpolation). We minimised the expression

$$\chi^2 = \sum_i \frac{(y_i - \langle \mathcal{B}_z \rangle\, x_i - b)^2}{\sigma_i^2}$$

where, for each spectral point i, $y_i = (V/I)_i$, $x_i = -g_{\rm eff} C_z \lambda_i^2 (1/I \times {\rm d}I/{\rm d}\lambda)_i$, and b is a constant term that,

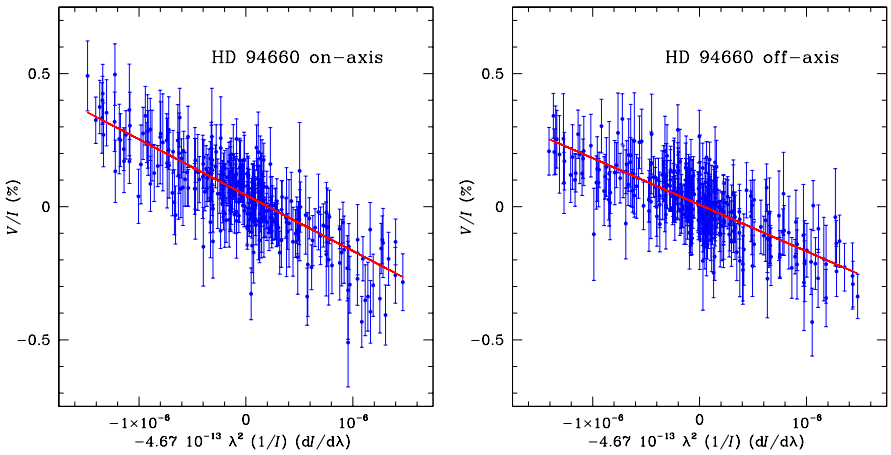

Fig. 3. The slope of the solid line (obtained via a least-square fit to the observed data) is proportional to the star's mean longitudinal field. For the magnetic star HD 94660 observed on-axis (left panel) we measured $\langle \mathcal{B}_z \rangle = -2085 \pm 85$ G. The fit to the data taken off-axis (i.e., with a 180″ telescope offset to the North), shown in the right-panel, leads to $\langle \mathcal{B}_z \rangle = -1735 \pm 85$ G.

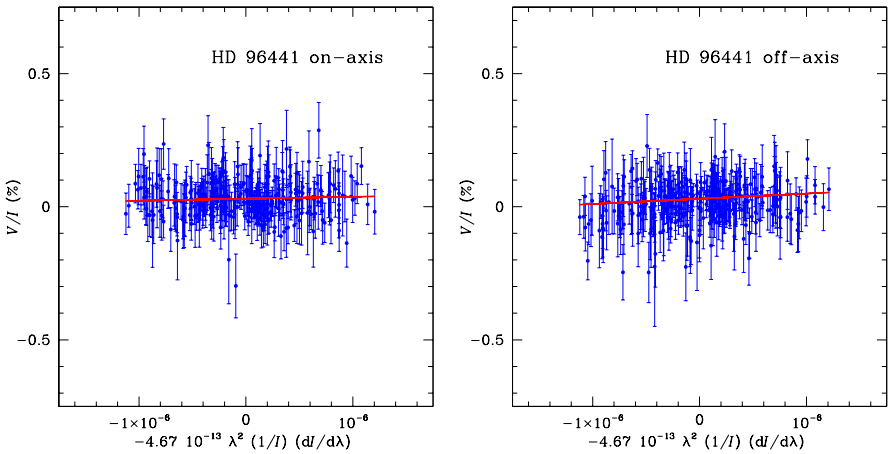

Fig. 4. As Fig. 3, for the star HD 96441. Left panel shows the fit to the data taken on-axis ($\langle \mathcal{B}_z \rangle = +70 \pm 80$ G), right panel refers to the data taken off-axis (i.e., with a 180″ telescope offset to the South, $\langle \mathcal{B}_z \rangle = +190 \pm 80$ G). There is no magnetic field detection.

Table 1. Determinations of the mean longitudinal magnetic field of HD 94660 from different spectral regions, and from spectra taken on- and off-axis. The corresponding HJDs are 24551991.499, and 2451991.513 for the on-axis and off-axis observations, respectively.

Wavelength regions	$\langle \mathcal{B}_z \rangle$ (G) on-axis	$\langle \mathcal{B}_z \rangle$ (G) off-axis
Hβ	-2070 ± 185	-2140 ± 190
Hγ	-1785 ± 220	-1820 ± 210
Hδ	-1800 ± 240	-1665 ± 245
Hϵ	-2005 ± 255	-1630 ± 250
H8	-2670 ± 290	-1330 ± 280
H9	-2030 ± 320	-1270 ± 320
H10	-2315 ± 315	-1285 ± 315
H11	-2595 ± 430	-2115 ± 440
H12	-2705 ± 520	-2860 ± 490
H13	-2290 ± 590	-1530 ± 550
H14	-2600 ± 790	-1100 ± 890
H15	-2610 ± 1200	-3790 ± 1150
H16	-3400 ± 2460	-575 ± 2620
All Balmer lines from Hβ to H16	-2085 ± 85	-1735 ± 85
Full wavelength range 3700−5750 Å	-2260 ± 65	-2015 ± 70
Metal lines only	-2110 ± 100	-2130 ± 110

assuming that Eq. (1) is correct, approximates the fraction of instrumental polarization not removed after the application of Eq. (2) to the observations (in this sense, the constant b can be defined as "residual" instrumental polarization). For each spectral point i, the derivative of Stokes I with respect to wavelength was evaluated as

$$\left(\frac{\mathrm{d}I}{\mathrm{d}\lambda}\right)_{\lambda=\lambda_i} = \frac{N_{i+1} - N_{i-1}}{\lambda_{i+1} - \lambda_{i-1}}$$

where N_i is the photon count at wavelength λ_i. The estimates for the errors on the parameters a and b (hence the errors on $\langle \mathcal{B}_z \rangle$) are given by the diagonal elements of the inverse of the χ^2 matrix.

The validity of Eq. (1) is limited to unblended lines formed in the weak-field regime. In fact, our spectrum must include hundreds of metallic lines, many of which are blended with H lines, and it is not obvious a priori to what extent the determination of the mean longitudinal field could depend upon the wavelength region. On the other hand, the fact that our observations span a large interval of wavelength offers us the opportunity to derive the mean longitudinal field from different spectral lines. We thus decided to use different criteria for the selection of spectral regions in which to apply Eq. (1), and then to compare the results.

We first determined the longitudinal field considering only those pixels within wavelength windows around

individual Balmer lines. We then derived the longitudinal field considering all Balmer lines simultaneously. Then, in order to obtain a rough estimate of the impact of blends with metallic lines on the determinations of the longitudinal field, we considered *all* data points from 3700 Å to 5750 Å (i.e., including all H Balmer lines and all metallic lines). We set the Landé factor $g_{\rm eff}$ to 1 for all lines, although this is appropriate only for H Balmer lines[2]. Finally, we considered the wavelength intervals 4400−4800 Å and 4900−5750 Å, which include metal lines *only*. For this experiment we set $g_{\rm eff} = 1.2$, a value representative of the average Landé factor for synthetic spectra of Ap stars. We repeated the measurements both for on-axis and off-axis observations. For HD 94660, the results of these experiments are summarised in Table 1, and are commented upon in the following.

From each H Balmer line (with the exception of those at $\lambda < 4100$ Å observed off-axis, see below), we obtained a determination of the mean longitudinal field consistent with the value expected from previous studies of the same star (obtained with different techniques). The consistency of the determination of the longitudinal field from the different Balmer lines demonstrates that, to first order, the incorrect physics underlying Eq. (1) does not introduce significant differences between magnetic field values obtained from different lines. Furthermore, we did not find evidence for systematic variations of the relation between V/I and $\mathrm{d}I/\mathrm{d}\lambda$ with the location in the line wing. Note however that the fact that this is true for a slowly rotating star does not guarantee that it is also valid for a fast rotator.

The error associated with the determinations of the longitudinal field obtained from individual Balmer lines is larger for Balmer lines at shorter wavelengths than for lines at longer wavelengths. This is due to the fact that the Zeeman effect increases as λ^2; thus the magnetic field is better detected at longer wavelengths than at shorter wavelengths. Furthermore, the photon count rate (and thus the S/N) decreases sharply at wavelengths shorter than about 4000 Å. Note also that Balmer lines from H10 to H16 are all mutually blended, which further hampers the determination of the mean longitudinal field.

At wavelengths blueward of Hδ, the determination of the longitudinal field from off-axis observations is systematically smaller (in absolute value) than that obtained from the observations taken at the field center. This is fully consistent with the fact that, at shorter wavelengths, we observed a smaller polarization signal in off-axis observations than in observations taken on-axis. It should be noted that the observed systematic discrepancy between determinations of the mean longitudinal field from observations on-axis versus off-axis confirms that the associated polarization discrepancy is not associated with a difference in the resolving power of the instrument, since it can be shown that the determination of the longitudinal field from spectropolarimetry of Balmer lines is independent of the spectral resolution (Landstreet 1982).

Figure 3 shows the best fit obtained by applying Eq. (1) to all Balmer lines. The reduced value of the χ^2 was 1.1 and 1.0 for the data taken on- and off-axis, respectively. We deem the corresponding $\langle \mathcal{B}_z \rangle$ value obtained from on-axis measurements, -2085 ± 85 G, our most accurate estimate of the longitudinal field. The value of -1735 ± 85 G obtained from the measurements off-axis is strongly biased by the depolarization observed at shorter wavelengths.

The outcome of the application of Eq. (1) to a wavelength interval including all Balmer lines *and* all metallic lines is a determination of longitudinal field fairly consistent with that obtained by carefully selecting the interval wavelengths around Balmer lines only (see Table 1). This suggests that in the wavelength regions around Balmer lines, the overall spectropolarimetric features are dominated by the Balmer lines themselves, and blends with metal lines have in fact little impact on the determination of the longitudinal field via Eq. (1).

The determination of mean longitudinal field through the application of Eq. (1) to *metallic lines* should be in principle strongly hampered by the fact that, in the photosphere of HD 94660, metallic lines do not form in the weak-field regime, nor can one safely assume that they are unblended. As a matter of fact, this experiment lead to an unexpected result, i.e., a $\langle \mathcal{B}_z \rangle$ measurement fairly consistent with that obtained from the analysis of H Balmer lines. We measured $\langle \mathcal{B}_z \rangle - 2110 \pm 100$ G from the measurements on-axis, and $\langle \mathcal{B}_z \rangle = -2130 \pm 110$ G from the spectra taken off-axis. Possibly, this consistency is due to a statistical phenomenon, i.e., deviations from the weak-field approximation for many metallic lines are compensated for on average, but this should be further investigated by means of numerical simulations and applications to other stars. This task is outside the scope of the present paper. However, it should be noted that the analysis of the metal lines do provide a remarkably robust second mean of determining the field, confirming the results of the analysis of the Balmer lines.

The value of the additional constant b allowing for instrumental polarization was found to be about +0.04% for the data on axis, and five times smaller than this value for the data taken off-axis, nearly independent of the actual wavelength interval considered for the least-square fit.

Mean longitudinal field determinations of HD 94660 were previously obtained by means of the photopolarimetric technique on the Hα Balmer line (Borra & Landstreet 1975) and on the Hβ Balmer line (Bohlender et al. 1993), while determinations were obtained using the "photographic" techniques on metallic lines by Mathys (1994) and by Mathys & Hubrig (1997). Further $\langle \mathcal{B}_z \rangle$ "photographic" measurements, to be published by Mathys et al. (in preparation), were used in the study of Landstreet & Mathys (2000). All measurements are shown in Fig. 5, which shows that our determination of the mean

[2] In the past it was commonly assumed that the Landé factor of H Balmer line was *about* 1. In fact, Casini & Landi Degl'Innocenti (1994) have shown that for H Balmer line $g_{\rm eff}$ is *exactly* equal to 1.

longitudinal field from all Balmer lines (represented by a filled circle) is consistent with the data obtained using other techniques by different authors.

In HD 96441, no magnetic field is detected from our data, nor to our knowledge has a field been detected in other works. From the analysis of all Balmer lines via Eq. (1) we obtained $\langle \mathcal{B}_z \rangle = +70 \pm 80\,\mathrm{G}$, and $\langle \mathcal{B}_z \rangle = +190 \pm 80\,\mathrm{G}$ for the observations on-axis and off-axis, respectively, with a value of the reduced $\chi^2/\nu = 1.0$ in both cases (see Fig. 3). It should be noted that a simple constant term b_0 provides a fit to our data with $\chi^2/\nu = 1.1$, i.e., nearly equivalent to the fit obtained through a first-order polynomial. The value of the constant b_0 obtained from the best-fit is about +0.03% for both on-axis and off-axis observations. This value is fully consistent with the value b obtained through a fit with a first-order polynomial to the data of the same star, and also with the value b obtained from the analysis of the on-axis data of the magnetic star HD 94660. We conclude that the "residual" instrumental *circular* polarization is less than few units in 10^{-4} at the center, top and bottom of the CCD field. This value is similar to that estimated in the *FORS* manual for the instrumental *linear* polarization. It should be noted that the impact of the instrumental polarization is kept to a minimal level thanks to the observing strategy described in Sect. 3. On the other hand, due to the nature of the cross-talk effect, for strongly linearly polarized sources, instrumental polarization could be found higher than estimated in this work.

Summarising, the determination of the longitudinal field from the Zeeman analysis of many Balmer lines using *FORS1* appears to be a fairly robust technique, although attention should be paid in the case of spectra taken off-axis, where, in order to obtain a precise $\langle \mathcal{B}_z \rangle$ measurement, it might be safer to discard from the Zeeman analysis those Balmer lines recorded at the very corners of the CCD (that however can still be used for *detection* of magnetic field). It should also be borne in mind that the *real* error associated with our estimates of $\langle \mathcal{B}_z \rangle$ is probably somewhat larger than the *formal* error obtained via the least-square technique, since considerations coming from the theory of line formation in magnetic photospheres suggest that the application of Eq. (1) to hydrogen lines should be regarded with some caution even in the weak-field regime (Mathys et al. 2000).

5. Discussion and conclusions

The results of our experiment permit us to roughly estimate that, for stars with spectral lines similar to HD 94660 and of magnitude V observed with 0.8″ seeing conditions, the longitudinal magnetic field can be measured with a formal error σ (in G) given a total exposure time (in seconds)

$$t = 20 \times 10^{(V-6)/2.5} \left(\frac{100}{\sigma}\right)^2. \quad (3)$$

For instance, a 400 G longitudinal field in a 13th magnitude star can be detected at a 3-σ confidence level with an exposure time of about 2 hours. However, note that Eq. (3) does not account for overheads due to telescope pointing, active optics, instrument set up, and (multiple) CCD readouts, which may amount altogether to as much as 15–20 min. Detection of magnetic fields in hotter stars (thus with weaker H Balmer lines) would probably require a slightly longer exposure time than that predicted with Eq. (3).

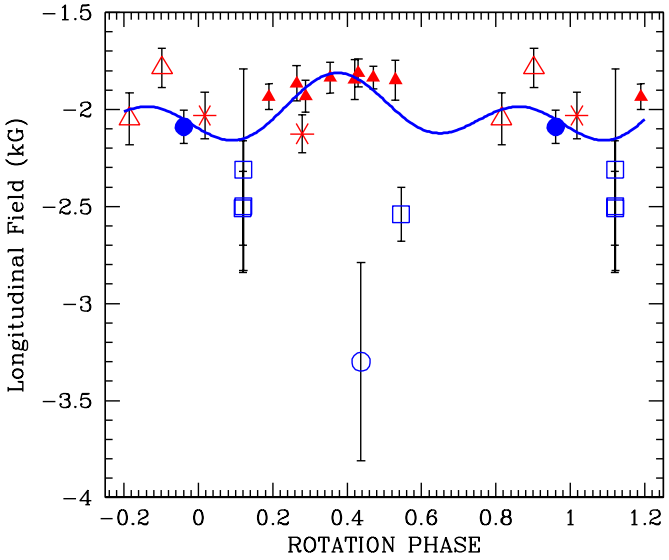

Fig. 5. Observations of the mean longitudinal magnetic field of HD 94660. Symbols are as follows: the empty circle represents the observation obtained via photopolarimetry of the Hα line by Borra & Landstreet (1975), empty squares those obtained via photopolarimetric techniques on Hβ by Bohlender et al. (1993). Asterisks show the measurements obtained with the photographic techniques by Mathys (1994), empty triangles those obtained by Mathys & Hubrig (1997) and filled triangles those presented in Landstreet & Mathys (2000). Our determination (obtained from all Balmer lines from Hβ to H16) is represented with a filled circle. The solid line is the best-fit to all observations obtained with a second-order Fourier expansions. For the stellar period we have assumed $P = 2764$ d (Landstreet & Mathys 2000). The zero phase point is at JD = 2446500.0.

On the other hand, detection of circular polarization in H Balmer lines is virtually unaffected by rotational Doppler broadening, so that *detecting* magnetic field with the proposed technique can be performed with little decrease in efficiency even for stars with very large $v_e \sin i$. Note however that for very fast rotators ($v_e \sin i \gtrsim 200\,\mathrm{km\,s^{-1}}$), some correlation between Doppler effect of various parts of the stellar surface and different strength and orientation of the field at these various locations could show through in the line profiles, yielding different values of the longitudinal field derived from different places in the line wings. Therefore, some caution may be required in the determination of the actual $\langle \mathcal{B}_z \rangle$ value. (One may think to "divide" the lines in several regions and to derive a field value independently for each of them, but this

would require even higher S/N than that needed using all the photons in the whole line for a single determination.)

It should be noted that *FORS1* has a multi-object mode which permits one to observe, in spectropolarimetry, up to nine stars at once. This mode can dramatically increase the efficiency of telescope time, e.g., for cluster studies. In case of multi-object applications, one may prefer a different instrument setup than what adopted in the present study, i.e., *GRISM 600 R* may be a better choice than *GRIMS 600 B*, due to the dependence of achieved wavelength coverage on the position of the target in the focal plane. The former grism spans a wavelength interval *centred* at Hα, whereas the latter spans the stellar spectrum from the Balmer jump up to about 5800 Å. For a slit positioned so that its image is projected on the CCD centre, the spectrum obtained with *GRIMS 600 B* is recorded in the left half side of the CCD. For cluster studies, this would reduce the useful field of view of *FORS1* to about half of its effective size (which is $6.8' \times 6.8'$). Finally, one should take into account that the depolarization observed off-axis will affect the precision of magnetic field measurements in stars observed at the edges of the field of view, although it will not significantly affect the possibility of detecting the presence of magnetic field.

In comparison, what are the limits and the advantages of using *FORS1* at the *VLT* for detecting magnetic fields in upper main sequence stars?

Most stellar spectropolarimeters of the present generation have been designed for application of the photographic technique through high-resolution observations of metallic lines. Examples of such instruments are the MuSiCoS (Donati et al. 1999) and ESPaDOnS (this latter is scheduled to see first light in late 2002, see Donati et al. 1998) spectropolarimeters. These tools are very effective for studies of cooler ($T_{\rm eff} \lesssim 20\,000$ K) stars with moderate ($v \sin i \lesssim 50$ km s^{-1}) rotation (e.g. Wade et al. 2000), where one can easily detect hundreds of metallic lines, thus obtaining a very high S/N per pixel is not a critical issue as for spectropolarimetry of H Balmer lines. However, the efficiency of high-resolution spectropolarimetry of metallic lines declines rapidly at higher temperatures (i.e. sparser line spectra) and more rapid rotation rates. Furthermore, the available instruments operate (or will operate, in the case of ESPaDOnS) on relatively small telescopes (the 2 m Telescope Bernard Lyot and the 3.6 m Canada-France-Hawaii Telescope, respectively). Therefore, spectropolarimetry of H Balmer lines with *FORS1* represents a tool for selection-free detection of ordered magnetic fields that is much more efficient than high-resolution spectropolarimetry with other instruments. On the other hand, a major limitation of magnetometry with *FORS1* is associated with the limited resolving power, hence lack of detailed information about the distribution of the magnetic field over the stellar disk. Therefore *FORS1* will never be the instrument of choice for the *detailed* modelling of magnetic field structures of upper main sequence stars.

In summary, we have tested a technique using measurements of circular polarization in Balmer lines with *FORS1* at the *VLT*, aimed at determining the longitudinal magnetic field $\gtrsim$300 G in upper main sequence stars. Because it is not strongly affected by either rotation or effective temperature, as well as thanks to *FORS1*'s multi-object mode, this technique is dramatically superior to high-resolution spectropolarimetry of metallic lines with any other current or planned instrument for performing selection-free surveys of magnetic fields in tepid and hot stars, especially those resident in clusters and associations.

Acknowledgements. Observations were obtained thanks to DDT 266.D-5649. GAW acknowledges research support from the Royal Military College of Canada Principal's Discretionary Fund. JDL acknowledges research support from the Natural Sciences and Engineering Research Council of Canada. We would like to thank Jason Spyromilio for very useful discussions.

References

Angel, J. R. P., & Landstreet, J. D. 1970, ApJ, 160, L147
Babcock, H. W. 1947, ApJ, 105, 105
Babcock, H. W. 1958, ApJS, 3, 141
Bohlender, D. A., Landstreet, J. D., & Thompson, I. B. 1993, A&A, 269, 355
Borra, E. F., & Landstreet, J. D. 1975, PASP, 87, 961
Borra, E. F., & Landstreet, J. D. 1980, ApJS, 42, 421
Casini, R., & Landi Degl'Innocenti, E. 1994, A&A, 291, 668
Donati, J.-F., Catala, C., Wade, G. A., et al. 1999, A&AS, 134, 149
Donati, J.-F., Catala, C., & Landstreet, J. D. 1998, in Proc. of the fifth CFHT user's meeting, 50
Gomez, A. E., Luri, X., Grenier, S., et al. 1998, A&A, 336, 953
Johns-Krull, C. M., Valenti, J. A., & Koresko, C. 1999, ApJ, 516, 900
Kemp, J. C., Swedlund, J. B., Landstreet, J. D., & Angel, J. R. P. 1970, ApJ, 161, 77
Landi Degl'Innocenti, E. 1992, in Solar observations: Techniques and interpretation, ed. F. Sánchez, M. Collados, & M. Vázquez (Cambridge Univ. Press), 71
Landstreet, J. D. 1982, ApJ, 258, 639
Landstreet, J. D., & Mathys, G. 2000, A&A, 359, 213
Leroy, J. L. 2000, A&AS, 101, 551
Mathys, G. 1994, A&AS, 108, 547
Mathys, G., & Hubrig, S. 1997, A&AS, 124, 475
Mathys, G., Stehlé, C., Brillant, S., & Lanz, T. 2000, A&A, 358, 1151
Putney, A. 1997, ApJS, 112, 527
Robinson, R. D., Worden, S. P., & Harvey, J. V. 1980, ApJ, 236, L155
Schmidt, G. D., & Smith, P. S. 1995, ApJ, 448, 305
Semel, M., Donati, J.-F., & Rees, D. E. 1993, A&A, 278, 231
Seifert, W., Appenzeller, I., Fürtig, W., et al. 2000, Commissioning of the FORS instruments at the ESO VLT, SPIE, 4008, 96
Szeifert, T., Böhnhardt, H. 2001, FORS1+2 User Manual 2.2; ESO document VLT-MAN-ESO-13100-1543
Wade, G. A., Donati, J.-F., Landstreet, J. D., & Shorlin, S. L. S. 2000, MNRAS, 313, 851